Available online at www.qu.edu.iq/journalcm
JOURNAL OF AL-QADISIYAH FOR COMPUTER SCIENCE AND MATHEMATICS
ISSN:2521-3504(online) ISSN:2074-0204(print)

Influence of MHD on mixed convective heat and mass transfer analysis for the peristaltic transport of viscoplastic fluid with porous medium in tapered channel

Mohammed Ali Murad[a,b,*] , Ahmed M. Abdulhadi[b]

[a]*Department of Mathematics, College of Basic Education, University of Diyala, Diyala, Iraq. E-mail: mindelawy66@yahoo.com*
[b]*Department of Mathematics, College of Science, University of Baghdad, Baghdad, Iraq. E-mail: ahm6161@yahoo.com*

ARTICLE INFO

Article history:
Received: 12 /12/2020
Rrevised form: 21 /12/2020
Accepted : 10 /01/2021
Available online: 11 /01/2021

Keywords:

Magnetic field, Viscoplastic fluid, Perturbation method , Peristaltic transport.

ABSTRACT

In this paper, the influence of magnetohydrodynamic (MHD) on a mixed convective heat and mass transfer analysis for the peristaltic transport of viscoplastic fluid in a non-uniform two dimensional tapered asymmetric channel with porous medium is investigated. The governed equations that described the motion of flow are simplified under assumptions of low Reynolds number and long wavelength. These equations are solved by mean of the regular perturbation method which is restricted to the smaller values of Bingham and Grashof numbers. Series solution for the axial velocity, temperature and concentration distribution have been computed. The flow quantities have been illustrated graphically for different interesting parameters. The trapping phenomena is also examined graphically.

MSC. 41A25; 41A35; 41A36.

DOI : https://doi.org/10.29304/jqcm.2020.12.4.728

1. Introduction

Peristaltic is a phenomenon of fluid transport induced by progressive of sinusoidal waves along the flexible walls of channels. This mechanism widely occurs in many industrial and biomedical application such as flow of lymph through lymphatic vessels, swallowing of food through esophagus, urine flow from the kidney to bladder, blood circulation in small blood vessels etc. Many of the physiological fluid (lymph, blood etc.) are noted to be non-Newtonian in nature. Many modern biomedical and mechanical instruments like blood pumps, the roller and finger pumps and heart-lung machines have been designed on the principle of peristaltic. In recent years, the combined effected of heat and mass transfer on peristaltic transport of non-Newtonian fluid in present of magnetic field receive considerable attentions due to its application in biomedical sciences [1-3]. Many researcher have been made theoretical analysis and various experimental to understand the peristaltic flow in both physiological and mechanical phenomenon under various assumption. Srinivas and Kothandapani [4] investigated the influence of heat and mass transfer on MHD peristaltic flow through porous space with compliant walls. Effect of heat and mass transfer on peristaltic flow of a Bingham fluid in the presence of inclined magnetic field and channel with different wave forms is studied by Akram et al. [5]. Ramesh [6] discussed the influence of heat and mass transfer on peristaltic flow of a couple stress fluid through porous medium in

∗Corresponding author *Mohammed Ali Murad, Ahmed M. Abdulhadi*

Email addresses: *mindelawy66@yahoo.com , ahm6161@yahoo.com*

Communicated by : Alaa Hussien Hamadi

the presence of inclined magnetic field in an inclined asymmetric channel. The effect of wall properties on the convective peristaltic transport of a conducting Bingham fluid through porous medium is examined by Satyanarayana et al. [7]. Lakshminarayana et al. [8] studied the peristaltic slip flow of a Bingham fluid in an inclined porous conduit with Joule heating. Adnan and Abdulhadi [9] analyzed the effect of a magnetic fluid on peristaltic transport of Bingham plastic fluid in a symmetric channel. Murad and Abdualhadi [10] studied the influence of heat and mass transfer on peristaltic transport of viscoplastic fluid in presence of magnetic field through symmetric channel with porous medium.

In this paper, the influence of MHD on mixed convective heat and mass transfer analysis for the peristaltic transport of viscoplastic fluid with porous medium in tapered channel is investigated under the assumption of low Reynolds number and long wavelength. The expression of velocity, temperature, concentration are obtained by using perturbation method. The impact of different physical parameters that appear in the problem are illustrated through graphs. Furthermore trapping phenomenon is also analyzed in detail.

2. Mathematical Formulation

Consider a peristaltic transport of an incompressible MHD viscoplastic fluid in a non-uniform two dimensional tapered asymmetric channel of width $(a_1 + a_2)$ with porous medium. Figure (1) gives the schematic diagram of the asymmetric channel. The flow is generated by propagation of wave on the channel walls train moving ahead with constant speed c, but with different wave amplitudes, phase angle and channel widths. Let $\bar{H}_1$ and $\bar{H}_2$ be the right side wall and the left side wall respectively in the stationary frame of reference $(\bar{X}, \bar{Y})$. The uniform magnetic field is applied in Y-direction to study the effect of it on the fluid flow. Electric field is absent. Heat and mass transfer studied through convective condition. The geometries of the channel walls are given by [11,12]

$$\bar{Y} = \bar{H}_1(\bar{X}, \bar{t}) = a_1 + \bar{b}\bar{X} + \bar{\phi}_1 \cos\left(\frac{2\pi}{\lambda}(\bar{X} - c\bar{t})\right) \tag{1}$$

for the right hand side wall,

$$\bar{Y} = \bar{H}_2(\bar{X}, \bar{t}) = -a_2 - \bar{b}\bar{X} - \bar{\phi}_2 \cos\left(\frac{2\pi}{\lambda}(\bar{X} - c\bar{t}) + \bar{\varphi}\right) \tag{2}$$

for the left hand side wall,

where $\bar{b}$ is the non-uniform parameter, $\bar{\phi}_1$ and $\bar{\phi}_2$ are the wave amplitudes, λ is the wavelength, $\bar{t}$ is the time, $\bar{\varphi}$ is the phase difference which varies in the range $0 \le \bar{\varphi} \le \pi$. Moreover $\bar{\varphi} = 0$ corresponds to the symmetric channel with waves out of phase and $\bar{\varphi} = \pi$ represents that the wave is in phase. Further $a_1, a_2, \bar{\phi}_1, \bar{\phi}_2$ and $\bar{\varphi}$ satisfy the condition $\bar{\phi}_1^2 + \bar{\phi}_2^2 + 2\bar{\phi}_1\bar{\phi}_1 cos\ \bar{\varphi} \le (a_1 + a_2)^2$ so that the walls not intersect with each other.

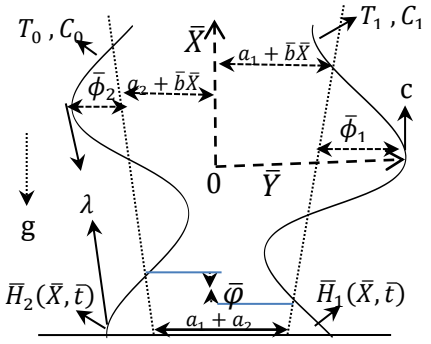

Fig. (1)- Schematic diagram of the asymmetric channel.

3. Basic and Constitutive Equations

Based on the above consideration, the basic governing equations that describe the flow in the present problem are given by [9,13]

equation of mass conservation

$$\nabla . \bar{\boldsymbol{V}} = 0, \tag{3}$$

motion equations (Navier-Stokes equations)

$$\rho \frac{d\bar{\boldsymbol{V}}}{dt} = \nabla . \bar{\boldsymbol{\sigma}} + \rho g \alpha (T - T_0) + \bar{\boldsymbol{J}} \times \bar{\boldsymbol{B}} - \frac{\eta}{\bar{k}_0} \bar{\boldsymbol{V}}, \tag{4}$$

energy equation

$$\rho C_p \frac{d\bar{T}}{dt} = \kappa \nabla^2 \bar{T} + \bar{\boldsymbol{\sigma}} . (\nabla \bar{\boldsymbol{V}}), \tag{5}$$

oncentration equation

$$\frac{d\bar{C}}{dt} = D_m \nabla^2 \bar{C} + \frac{D_m K_T}{T_m} \nabla^2 \bar{T}, \tag{6}$$

in which $\overline{\boldsymbol{V}}$ is the velocity, ρ is the density, $\frac{d}{dt}$ is the material time derivative, α is the coefficient of thermal expansion, $\bar{\boldsymbol{\sigma}}$ is the Cauchy stress tensor, g is the acceleration due to gravity, $\bar{\boldsymbol{J}} = \sigma'(\overline{\boldsymbol{V}} \times \overline{\boldsymbol{B}})$ is the current density, $\overline{\boldsymbol{B}} = (0, B_0, 0)$ is the magnetic field, σ' is the electrical conductivity, η is the viscosity, $\bar{k}_0$ is the permeability parameter of porous medium, $\nabla^2$is the Laplace operator, $\bar{T}$ is the temperature, κ is the thermal conductivity, C_p is the specific heat, $\bar{C}$ is the mass concentration, D_m is the coefficient of mass diffusion, K_T is the thermal diffusion ratio and T_m is the mean temperature.

The term $(\bar{\boldsymbol{\sigma}}.(\nabla\overline{\boldsymbol{V}}))$ in equation (5) can be compute from the definition of dot product of two tensor (if $B$and $\hat{B}$ are any two tensor then $B.\hat{B} = tra(B\hat{B})$). Let $\bar{U}$ and $\bar{V}$ be the velocity components along the $\bar{X}$ and $\bar{Y}$-directions respectively in the fixed frame, the velocity vector $\overline{\boldsymbol{V}}$ can be written as

$$\overline{\boldsymbol{V}} = (\bar{U}(\bar{X}, \bar{Y}, \bar{t}), \bar{V}(\bar{X}, \bar{Y}, \bar{t}), 0). \tag{7}$$

The Bingham plastic fluid is considered and the constitutive equations can be defined as [3,9]

$$\bar{\boldsymbol{\sigma}} = -\bar{P}I + \bar{\tau}, \tag{8}$$

$$\bar{\tau} = 2\eta D + 2\tau_0 \widetilde{D}, \tag{9}$$

in above equations, $\bar{\tau}$ is the extra tensor, , I is the identity tensor, $\bar{P}$ is the pressure while the rate of deformation tensor D and the tensor $\widetilde{D}$ are defined by

$$D = \frac{1}{2}(\nabla\bar{V} + (\nabla\bar{V})^T), \ \widetilde{D} = \frac{D}{\sqrt{2traD^2}}. \tag{10}$$

From equations (3)-(8), the governing equation in the fixed frame are given by

$$\frac{\partial\bar{U}}{\partial\bar{X}} + \frac{\partial\bar{V}}{\partial\bar{Y}} = 0, \tag{11}$$

$$\rho\left(\frac{\partial\bar{U}}{\partial\bar{t}} + \bar{U}\frac{\partial\bar{U}}{\partial\bar{X}} + \bar{V}\frac{\partial\bar{U}}{\partial\bar{Y}}\right) = -\frac{\partial\bar{P}}{\partial\bar{X}} + \frac{\partial\bar{\tau}_{\bar{X}\bar{X}}}{\partial\bar{X}} + \frac{\partial\bar{\tau}_{\bar{X}\bar{Y}}}{\partial\bar{Y}} + \rho g\alpha(T - T_0) - \sigma' B_0^2\bar{U} - \frac{\eta}{\bar{k}_0}\bar{U}, \tag{12}$$

$$\rho\left(\frac{\partial\bar{V}}{\partial\bar{t}} + \bar{U}\frac{\partial\bar{V}}{\partial\bar{X}} + \bar{V}\frac{\partial\bar{V}}{\partial\bar{Y}}\right) = -\frac{\partial\bar{P}}{\partial\bar{Y}} + \frac{\partial\bar{\tau}_{\bar{Y}\bar{X}}}{\partial\bar{X}} + \frac{\partial\bar{\tau}_{\bar{Y}\bar{Y}}}{\partial\bar{Y}} - \frac{\eta}{\bar{k}_0}\bar{V}, \tag{13}$$

$$\left(\frac{\partial\bar{T}}{\partial\bar{t}} + \bar{U}\frac{\partial\bar{T}}{\partial\bar{X}} + \bar{V}\frac{\partial\bar{T}}{\partial\bar{Y}}\right) = \kappa\left(\frac{\partial^2\bar{T}}{\partial\bar{X}^2} + \frac{\partial^2\bar{T}}{\partial\bar{Y}^2}\right) + \bar{\tau}_{\bar{X}\bar{X}}\frac{\partial\bar{U}}{\partial\bar{X}} + \bar{\tau}_{\bar{X}\bar{Y}}\frac{\partial\bar{V}}{\partial\bar{X}} + \bar{\tau}_{\bar{Y}\bar{X}}\frac{\partial\bar{U}}{\partial\bar{Y}} + \bar{\tau}_{\bar{Y}\bar{Y}}\frac{\partial\bar{V}}{\partial\bar{Y}}, \tag{14}$$

$$\left(\frac{\partial\bar{C}}{\partial\bar{t}} + \bar{U}\frac{\partial\bar{C}}{\partial\bar{X}} + \bar{V}\frac{\partial\bar{C}}{\partial\bar{Y}}\right) = D_m\left(\frac{\partial^2\bar{C}}{\partial\bar{X}^2} + \frac{\partial^2\bar{C}}{\partial\bar{Y}^2}\right) + \frac{D_m K_T}{T_m}\left(\frac{\partial^2\bar{T}}{\partial\bar{X}^2} + \frac{\partial^2\bar{T}}{\partial\bar{Y}^2}\right). \tag{15}$$

The corresponding boundary conditions are

$$\left.\begin{aligned} \bar{U} = 0 \ , \ \bar{T} = \bar{T}_1 \ , \ \bar{C} = \bar{C}_1 \quad at\ \bar{Y} = \bar{H}_1 \\ \bar{U} = 0 \ , \ \bar{T} = T_0 \quad , \ \bar{C} = C_0 \quad at\ \bar{Y} = \bar{H}_2 \end{aligned}\right\}. \tag{16}$$

In view of equations (9) and (10), the components of extra stress tensor in the fixed frame becomes

$$\bar{\tau}_{\bar{X}\bar{X}} = 2\eta\frac{\partial\bar{U}}{\partial\bar{X}} + \frac{2\bar{\tau}_0\frac{\partial\bar{U}}{\partial\bar{X}}}{(2\left(\frac{\partial\bar{U}}{\partial\bar{X}}\right)^2 + \left(\frac{\partial\bar{U}}{\partial\bar{Y}} + \frac{\partial\bar{V}}{\partial\bar{X}}\right)^2 + \left(\frac{\partial\bar{V}}{\partial\bar{Y}}\right)^2)^{\frac{1}{2}}},$$

$$\bar{\tau}_{\bar{X}\bar{Y}} = \bar{\tau}_{\bar{Y}\bar{X}} = \eta(\frac{\partial\bar{U}}{\partial\bar{Y}} + \frac{\partial\bar{V}}{\partial\bar{X}}) + \frac{\bar{\tau}_0(\frac{\partial\bar{U}}{\partial\bar{Y}} + \frac{\partial\bar{V}}{\partial\bar{X}})}{(2\left(\frac{\partial\bar{U}}{\partial\bar{X}}\right)^2 + \left(\frac{\partial\bar{U}}{\partial\bar{Y}} + \frac{\partial\bar{V}}{\partial\bar{X}}\right)^2 + \left(\frac{\partial\bar{V}}{\partial\bar{Y}}\right)^2)^{\frac{1}{2}}},$$

$$\bar{\tau}_{\bar{Y}\bar{Y}} = 2\eta\frac{\partial\bar{V}}{\partial\bar{Y}} + \frac{2\bar{\tau}_0\frac{\partial\bar{V}}{\partial\bar{Y}}}{(2\left(\frac{\partial\bar{U}}{\partial\bar{X}}\right)^2 + \left(\frac{\partial\bar{U}}{\partial\bar{Y}} + \frac{\partial\bar{V}}{\partial\bar{X}}\right)^2 + \left(\frac{\partial\bar{V}}{\partial\bar{Y}}\right)^2)^{\frac{1}{2}}}. \tag{17}$$

Peristaltic motion is unsteady phenomenon in nature but it can be assumed steady by using the transformation from the laboratory frame (fixed frame) $(\bar{X}, \bar{Y})$ to the wave frame (move frame) $(\bar{x}, \bar{y})$ which defined as [3,12]

$$\bar{x} = \bar{X} - c\bar{t} \ , \ \bar{y} = \bar{Y} \ , \ \bar{u}(\bar{x}, \bar{y}) = \bar{U}(\bar{X}, \bar{Y}, \bar{t}) - c \ , \bar{v}(\bar{x}, \bar{y}) = \bar{V}(\bar{X}, \bar{Y}, \bar{t}),$$

$$\bar{p}(\bar{x}, \bar{y}) = \bar{P}(\bar{X}, \bar{Y}, \bar{t}), \ \bar{T}(\bar{x}, \bar{y}) = \bar{T}(\bar{X}, \bar{Y}, \bar{t}), \ \bar{C}(\bar{x}, \bar{y}) = \bar{C}(\bar{X}, \bar{Y}, \bar{t}), \tag{18}$$

where $\bar{u}$, $\bar{w}$ and $\bar{p}$ are the velocity components and the pressure in the wave frame, respectively.

Now, we transform equations (1), (2) and (11)-(17) in wave frame with the help of equation (18) and normalize the resulting equations by using following non-dimensional quantities [3,12]

$$\left.\begin{aligned} \bar{x}=\lambda x\ ,\bar{y}=a_1 y\ ,\bar{u}=cu\ ,\bar{v}=cv\ ,\bar{t}=\frac{\lambda}{c}t\ ,\bar{p}=\frac{c\eta\lambda}{a_1^2}p,\\ Re=\frac{\rho a_1 c}{\eta}\ ,\bar{\phi}_1=a_1\phi_1\ ,\bar{\phi}_2=a_1\phi_2,\delta=\frac{a_1}{\lambda}\ ,\bar{H}_1=a_1H_1,\\ \bar{H}_2=a_1H_2,a=\frac{a_2}{a_1}\ ,Q^*=a_1c\Theta\ ,\bar{q}=a_1cF\ ,\bar{k}_0=a_1^2k_0\ ,\\ \bar{b}=\frac{a_1}{\lambda}b\ ,\bar{\tau}=\frac{c\,\eta}{a_1}\tau_{ij},\bar{\psi}=ca_1\psi\ ,\ \theta=\frac{\bar{T}-T_0}{T_1-T_0},\Omega=\frac{\bar{C}-C_0}{C_1-C_0},\\ Pr=\frac{C_p\eta}{\kappa},Ec=\frac{c^2}{C_p(T_1-T_0)},Sc=\frac{\eta}{\rho D_m}\ ,Sr=\frac{\rho D_m(T_1-T_0)K_T}{\eta T_m\,(C_1-C_0)},\\ A^2=M^2+\frac{1}{k_0},Bn=\frac{a_1\tau_0}{c\,\eta}\ ,M^2=\frac{\sigma' B_0^2 a_1^2}{\eta},Gr=\frac{\rho g\alpha\ a_1^2(T_1-T_0)}{c\,\eta}, \end{aligned}\right\} \quad (19)$$

to obtain

$$y=H_1(x)=1+bx+\phi_1 cos2\pi x\ , \quad (20)$$

$$y=H_2(x)=-a-bx-\phi_2\cos(2\pi x+\bar{\varphi})\ , \quad (21)$$

$$\delta\frac{\partial u}{\partial x}+\frac{\partial v}{\partial y}=0\ , \quad (22)$$

$$Re\left((u+1)\delta\frac{\partial u}{\partial x}+v\frac{\partial u}{\partial y}\right)=-\frac{\partial p}{\partial x}+\delta\frac{\partial \tau_{xx}}{\partial x}+\frac{\partial \tau_{xy}}{\partial y}+Gr\theta-A^2(u+1)\ , \quad (23)$$

$$Re\ \delta\left((u+1)\delta\frac{\partial v}{\partial x}+v\frac{\partial v}{\partial y}\right)=-\frac{\partial p}{\partial y}+\delta^2\frac{\partial \tau_{yx}}{\partial x}+\delta\frac{\partial \tau_{yy}}{\partial y}-\delta\frac{1}{k_0}v, \quad (24)$$

$$RePr\left((u+1)\frac{\partial \theta}{\partial x}+v\frac{\partial \theta}{\partial y}\right)=\left[\delta^2\frac{\partial^2\theta}{\partial x^2}+\frac{\partial^2\theta}{\partial y^2}\right]+EcPr\delta\frac{\partial u}{\partial y}\tau_{xx}+EcPr(\frac{\partial u}{\partial y}+\delta\frac{\partial v}{\partial x})\tau_{xy}+EcPr\frac{\partial v}{\partial y}\ \tau_{yy}\ , \quad (25)$$

$$Re\left((u+1)\frac{\partial \Omega}{\partial x}+v\frac{\partial \Omega}{\partial y}\right)=\frac{1}{Sc}\left[\delta^2\frac{\partial^2\Omega}{\partial x^2}+\frac{\partial^2\Omega}{\partial y^2}\right]+Sr\left[\delta^2\frac{\partial^2\theta}{\partial x^2}+\frac{\partial^2\theta}{\partial y^2}\right], \quad (26)$$

$$\left.\begin{aligned} u=-1\ ,\theta=1\ ,\Omega=1\quad at\ y=H_1\\ u=-1\ \ ,\ \ \theta=0,\ \Omega=0\quad aty=H_2 \end{aligned}\right\}, \quad (27)$$

and

$$\tau_{xx}=2\delta\frac{\partial u}{\partial x}+\frac{2Bn\delta\frac{\partial u}{\partial x}}{(2\delta^2\left(\frac{\partial u}{\partial x}\right)^2+\left(\frac{\partial u}{\partial y}+\delta\frac{\partial v}{\partial x}\right)^2+\left(\frac{\partial v}{\partial y}\right)^2)^{\frac{1}{2}}}\ ,$$

$$\tau_{xy}=\tau_{yx}=(\frac{\partial u}{\partial y}+\delta\frac{\partial v}{\partial x})+\frac{Bn(\frac{\partial u}{\partial y}+\delta\frac{\partial v}{\partial x})}{(2\delta^2\left(\frac{\partial u}{\partial x}\right)^2+\left(\frac{\partial u}{\partial y}+\delta\frac{\partial v}{\partial x}\right)^2+\left(\frac{\partial v}{\partial y}\right)^2)^{\frac{1}{2}}},$$

$$\tau_{yy}=2\frac{\partial v}{\partial y}+\frac{2Bn\frac{\partial v}{\partial y}}{(2\delta^2\left(\frac{\partial u}{\partial x}\right)^2+\left(\frac{\partial u}{\partial y}+\delta\frac{\partial v}{\partial x}\right)^2+\left(\frac{\partial v}{\partial y}\right)^2)^{\frac{1}{2}}}\ , \quad (28)$$

in the above expressions, T_1 and T_0 are the temperature at the right side wall and the left side wall respectively whereas C_1 and C_0 denoted the concentration at the right side wall and the left side wall of the channel respectively. $\bar{\psi}$ is the stream function, δ is the dimensionless wave number, Re is the Reynolds number, Ec is the Eckert number, Pr is the Prandtl number, Sr is the Soret number, Sc is the Schmidt number, M is the Hartman number, Bn is the Bingham number, Gr is the Grashof number, Ω is the non-dimensional the concentration and θ is the temperature in the non-dimensional form.

Introduction of dimensionless stream function(ψ) by the relations $u=\psi_y$ and $v=-\delta\psi_x$ in equations (22)-(28) shows that the continuity equation satisfies identically while other equations subjected to $\delta \ll 1$ and $Re \ll 1$, yields

$$\frac{\partial p}{\partial x}=\frac{\partial}{\partial y}\tau_{xy}+Gr\theta-A^2(\psi_y+1), \quad (29)$$

$$\frac{\partial p}{\partial y}=0, \quad (30)$$

$$\frac{\partial^2\theta}{\partial y^2}=Br\tau_{xy}\psi_{yy}, \quad (31)$$

$$\frac{\partial^2\Omega}{\partial y^2}=-ScSr\frac{\partial^2\theta}{\partial y^2}, \quad (32)$$

$$\left.\begin{aligned} \psi_y=-1\ ,\theta=1\ ,\Omega=1\qquad at\ y=H_1\\ \psi_y=-1,\ \ \theta=0\ \ ,\ \Omega=0\qquad at\ y=H_2 \end{aligned}\right\}, \quad (33)$$

and

$$\tau_{xx}=\tau_{yy}=0,\ \tau_{xy}=\psi_{yy}+B_n, \quad (34)$$

where, $Br = EcPr$, is the Brinkman number.

By substituting equation (34) into equation (29) and deriving the result with respect to y, in view of equation (30), yields

$$\psi_{yyyy} + Gr\frac{\partial\theta}{\partial y} - A^2\psi_{yy} = 0. \tag{35}$$

From equation (31) and (34) we have

$$\theta_{yy} = Br\left(\psi_{yy}^2 + Bn\psi_{yy}\right) \tag{36}$$

4. Rate of Volume Flow

At any instant the volume flow rate in the fixed frame reference ($\bar{X}, \bar{Y}$) is given by

$$\bar{Q}(\bar{X},\bar{t}) = \int_{\bar{H}_2(\bar{X},\bar{t})}^{\bar{H}_1(\bar{X},\bar{t})} \bar{U}(\bar{X},\bar{Y},\bar{t})d\bar{Y}, \tag{37}$$

while the expression for the volumetric flow rate in the wave frame of reference ($\bar{x}, \bar{y}$) is defined as

$$\bar{q}(\bar{x}) = \int_{\bar{H}_2(\bar{x})}^{\bar{H}_1(\bar{x})} \bar{u}(\,\bar{x},\bar{y}\,)d\bar{y}. \tag{38}$$

Using equation (18) into equation (37) and making use of equation (38) we obtain the relation of the two fluxes as follows

$$\bar{Q} = \bar{q} + c\left(\bar{H}_1(\bar{x}) - \bar{H}_2(\bar{x})\right). \tag{39}$$

The average volume flow rate over the period time $T = (\frac{\lambda}{c})$ of the peristaltic wave at a fixed position $\bar{x}$ is defined as

$$Q^* = \frac{1}{T}\int_0^T \bar{Q}d\bar{t}. \tag{40}$$

Substituting equation (39) into equation (40), we have

$$Q^* = \bar{q} + ca_1 + ca_2 + 2c\bar{b}. \tag{41}$$

Using equation (19) ($\Theta = \frac{Q^*}{ca_1}, F = \frac{\bar{q}}{ca_1}$) into equation (41) we have

$$\Theta = F + 1 + a + 2b, \tag{42}$$

where F is the dimensionless volume flow rate in the wave frame defined by

$$F = \int_{H_2(x)}^{H_1(x)} \frac{\partial\psi}{\partial y}dy = \psi\left(H_1(x)\right) - \psi\left(H_2(x)\right), \tag{43}$$

then $\psi = \frac{F}{2}$ at the right wall and $\psi = -\frac{F}{2}$ at the left wall of the channel.

The non-dimension expression for pressure rise over one cycle of the wave is given by

$$\Delta P_\lambda = \int_0^1 \frac{\partial p}{\partial x}dx. \tag{44}$$

which is difficult to evaluate directly, so we used MATHEMATICA software to compute it numerically.

5. Solution of the Problem

In above equations, we have a system of non-linear partial differential equations which is difficult to solve it exactly. So, had to resort to the application of an approximation method, via the regular perturbation method to solve it. Let us expand stream function and the concentration for small values of Bingham number ($Bn \ll 1$) and the temperature for small values of Grashof number ($Gr \ll 1$) as follows

$$\begin{aligned}\psi &= \textstyle\sum_{i=0}^{\infty}(Bn)^i\,\psi_i + O(Bn^2),\\ \theta &= \textstyle\sum_{i=0}^{\infty}(Gr)^i\,\theta_i + O(Gr^2),\\ \Omega &= \textstyle\sum_{i=0}^{\infty}(Bn)^i\,\Omega_i + O(Bn^2).\end{aligned} \tag{45}$$

Inserting equation (45) into equations (32), (35) and (36) with the corresponding boundary conditions (equation (33)) and then collecting the coefficients of like power of Bn and Gr yields the zeroth and the first order systems.

5.1 Zeroth Order System

$$\psi_{0yyyy} - A^2\psi_{0yy} = 0, \tag{46}$$

$$\theta_{0yy} + Br\psi_{0yy}^2 = 0\,, \tag{47}$$

$$\Omega_{0yy} + ScSr\theta_{oyy} = 0\ , \tag{48}$$

with the corresponding boundary conditions

$$\left.\begin{aligned}\psi_0 = \frac{F}{2}, \psi_{0y} = -1\ , \theta_0 = 1\,, \Omega_0 = 1 \quad at\ y = H_1\\ \psi_0 = -\frac{F}{2}, \psi_{0y} = -1,\ \ \theta_0 = 0\,,\ \Omega_0 = 0 \quad at\ y = H_2\end{aligned}\right\}. \tag{49}$$

5.2 First Order System

$$\psi_{1yyyy} + \theta_{oy} - A^2\psi_{1yy} = 0\,, \tag{50}$$

$$\theta_{1yy} + 2Br\psi_{0yy}\psi_{1yy} + \psi_{1yy} = 0\,, \tag{51}$$
$$\Omega_{1yy} + ScSr\theta_{1yy} = 0\,, \tag{52}$$

with the corresponding boundary conditions

$$\left.\begin{array}{l} \psi_1 = 0, \psi_{1y} = 0\ , \theta_1 = 0\,, \Omega_1 = 0 \quad at\ y = H_1 \\ \psi_1 = 0, \psi_{1y} = 0,\ \ \theta_1 = 0\,,\ \Omega_1 = 0 \quad at\ y = H_2 \end{array}\right\}. \tag{53}$$

The final solution of the above systems (zeroth and first order) by using MATHEMATICA software with corresponding boundary conditions are

$$\begin{aligned}\psi = {} & \frac{\frac{e^{Ay}\mathrm{c1}}{A} + \frac{e^{-Ay}\mathrm{c2}}{A}}{A} + \mathrm{c3} + y\mathrm{c4} - \frac{1}{24A^5}(\mathrm{Br}(\mathrm{c2}^2 e^{-2Ay} - \\ & \mathrm{c1}^2 e^{2Ay} + 8A^3\mathrm{c1c2}y^3) - 12A^3 e^{-Ay}(\mathrm{c6}e^{Ay}y^2 + \\ & 2(e^{2Ay}\mathrm{c9} + \mathrm{c10}))) + \mathrm{c11} + y\mathrm{c12}\,,\end{aligned} \tag{54}$$

$$\begin{aligned}\theta = {} & \frac{\mathrm{Br}\left(-\frac{\mathrm{c2}^2 e^{-2Ay}}{2A} - \frac{\mathrm{c1}^2 e^{2Ay}}{2A} - 2A\mathrm{c1c2}y^2\right)}{2A} + \mathrm{c5} + y\mathrm{c6} \\ & -\frac{1}{216A^5}e^{-3Ay}(108A^3 e^{2Ay}(2\mathrm{c10} + 2\mathrm{c9}e^{2Ay} + \mathrm{c6}e^{Ay}y^2) - \\ & 8\mathrm{Br}^2(\mathrm{c2}^3 - \mathrm{c1}^3 e^{6Ay} + 9\mathrm{c1}^2\mathrm{c2}e^{4Ay}(-25 + 12Ay) + 9\mathrm{c1c2}^2 e^{2Ay} \\ & (25 + 12Ay)) + 9\mathrm{Br}e^{Ay}(-\mathrm{c2}^2 + \mathrm{c1}^2 e^{4Ay} + 48A\mathrm{c6}e^{Ay}(\mathrm{c2} + \mathrm{c1}e^{2Ay}) \\ & +24A^5(\mathrm{c1c10} + \mathrm{c2c9})e^{2Ay}y^2 + 4A^3(3\mathrm{c10c2} + 3\mathrm{c1c9}e^{4Ay} - \\ & 2\mathrm{c1c2}e^{2Ay}y^3))) + \mathrm{c13} + y * \mathrm{c14}\,,\end{aligned} \tag{55}$$

$$\begin{aligned}\Omega \quad = {} & \frac{1}{2}\mathrm{BrScSr}\left(\frac{\mathrm{c2}^2 e^{-2Ay}}{2A^2} + \frac{\mathrm{c1}^2 e^{2Ay}}{2A^2} + 2\mathrm{c1c2}y^2\right) + \mathrm{c7} + y\mathrm{c8} \\ & + \frac{1}{216A^5}e^{-3Ay}\mathrm{ScSr}(108A^3 e^{2Ay}(2\mathrm{c10} + 2\mathrm{c9}e^{2Ay} + \\ & \mathrm{c6}e^{Ay}y^2) - 8\mathrm{Br}^2(\mathrm{c2}^3 - \mathrm{c1}^3 e^{6Ay} + 9\mathrm{c1}^2\mathrm{c2}e^{4Ay}(-25 + 12Ay) + \\ & 9\mathrm{c1c2}^2 e^{2Ay}(25 + 12Ay)) + 9\mathrm{Br}e^{Ay}(-\mathrm{c2}^2 + \mathrm{c1}^2 e^{4Ay} + \\ & 48A\mathrm{c6}e^{Ay}(\mathrm{c2} + \mathrm{c1}e^{2Ay}) + 24A^5(\mathrm{c1c10} + \mathrm{c2c9})e^{2Ay}y^2 + \\ & 4A^3(3\mathrm{c10c2} + 3\mathrm{c1c9}e^{4Ay} - 2\mathrm{c1c2}e^{2Ay}y^3))) + \mathrm{c15} + y\mathrm{c16}\,,\end{aligned} \tag{56}$$

where $\mathrm{c}_i\,, i = 1,2, \ldots, 16$ are constants which are found by using the boundary conditions.

6. Results and Discussion

To study the effect of physical parameters such as Hartmann number (magnetic parameter) M, permeability parameter k_0, non-uniform parameter b, amplitudes wave of right (ϕ_1) and left (ϕ_2) walls ,Bingham number Bn, Brinkman number Br, phase angle $\bar{\varphi}$, Grashof number Gr, flow rate F, Schmit number Sc, and Soret numberSr, we have plotted the axial velocity u, temperature θ, concentration Ω, and trapping phenomenon in Figures (2-39). All figures are plotted for the values $M = 0.5, b = 0.2, k_0 = 2, Bn = 0.001, Br = 6, F = 1.4,\ \bar{\varphi} = {}^{\pi}/_{4}\,, \phi_1 = 3, \phi_2 = 2, x = 0.1,$ $Sc = 0.4$ and $Sr = 0.8$ using MATHEMATICA software.

6.1 Velocity Distribution u

Graphical results are displayed in order to see the behavior of parameters involved in the axial velocity u. The effect of different values of $M, F, b, k_0, \phi_1, \phi_2, \bar{\varphi}, Bn$ and Br on u are explained in figures (2-10). The behavior of velocity distribution is parabolic as seen in figures. Figure (2) shows the influence of M on u. It is noticed that with an increase of M, the axial velocity increases at the left and right part of the channel, however, it decreases at the central part of the channel. It observed from figure (3) that u increases by increasing in F whereas it decreases by increasing in b, as shown in figures (4). Figure (5) shows the impact of k_0 on u. It is noticed that at the left and right wall of the channel u decreases slowly with an increase of k_0, however at the central part of the channel u increases. Figure (6) explained that u increases near the right wall and the middle part of the channel and the situation is opposite at the left wall of the channel with an increase in ϕ_1. Figure (7) displays the effect of ϕ_2 on u. It is noticed that when an increase in ϕ_2, u increases at the left wall of the channel and merges from the central part to the rest of the channel (no effected). From figure (8) we noted that at an increase in $\bar{\varphi}$, u decreases at the left wall of the channel and merges from the central part to the right wall of the channel. Figure (9) illustrated the impact of Bn on u. It is observed that the increase in Bn lead to u decreases at the left wall of the channel, while u increasing at the middle portion and then gradually disappear as there is no effect on axial velocity near the right wall of the channel. From figure (10) observed that u do not change at an increasing in Br. One can observe a very good agreement of our results for M , F, ϕ_1, ϕ_2 and $\bar{\varphi}$ with those reported in Adnan and Abdulhadi [9]

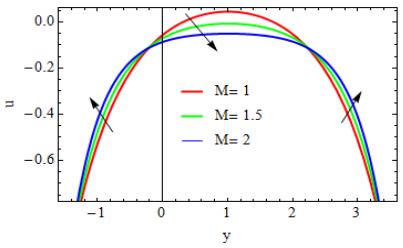

Fig. (2)- Effect of M on the axial velocity u

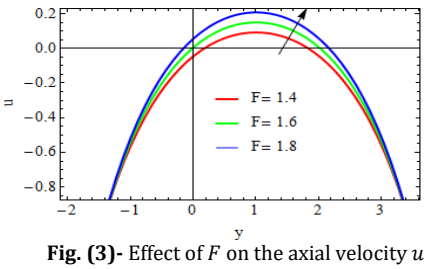

Fig. (3)- Effect of F on the axial velocity u

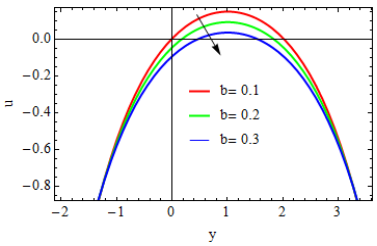

Fig. (4)- Effect of b on the axial velocity u

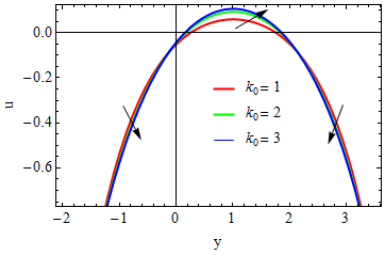

Fig. (5)- Effect of k_0 on the axial velocity u

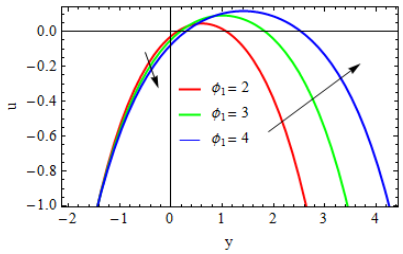

Fig. (6)- Effect of ϕ_1 on the axial velocity u

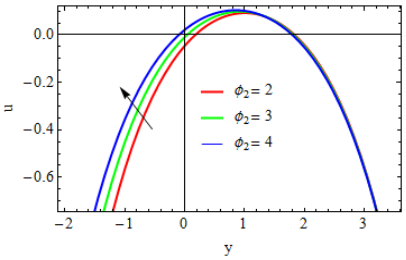

Fig. (7)- Effect of ϕ_2 on the axial velocity u

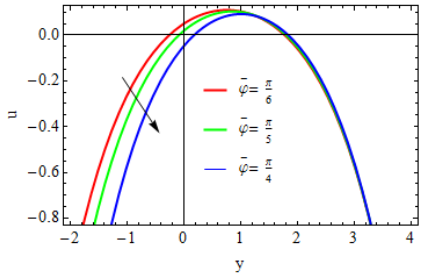

Fig. (8)- Effect of $\bar{\varphi}$ on the axial velocity u

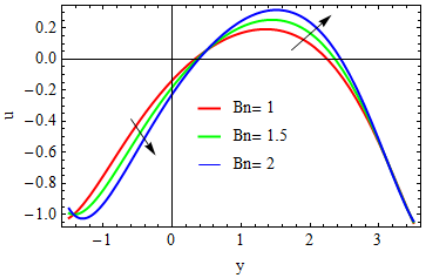

Fig. (9)- Effect of Bn on the axial velocity u

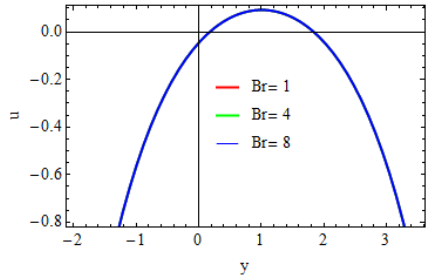

Fig. (10)- Effect of Br on the axial velocity u

6.2 Temperature Distribution θ

The variation in temperature profile for different values of involved parameters are illustrated in figures (11-19). Figure (11) shows that the impact of M on θ. It is noticed that θ exhibits oscillating behavior with an increase in M. It is concluded from figure (12), θ increases in the central region and decreases near the channel walls for increasing in Br, but opposite behavior is occurring with the increase in b, as shown in figure (13). Figures (14-16) shown θ increases by increasing in k_0, Gr and F. Figure (17) illustrated that θ increases near the right wall and the middle part of the channel and then gradually disappear as there is no effect on θ to the rest of the channel with an increase in ϕ_1. Figure (18) explained the effect of ϕ_2 on θ. It is noticed that when an increase in ϕ_2, the temperature increases at the left wall of the channel and merges from the central part to the rest of the channel (no effected). From figure (19) we noted that at an increase in $\bar{\varphi}$, θ decreases at the left wall of the channel and merges from the central part to the right wall of the channel. The effects of Br, Gr, F, ϕ_1, ϕ_2 and $\bar{\varphi}$ are consistent with the results analyzed in previous studies (Adnan and Abdulhadi [9] and Ali and Asghar [3]).

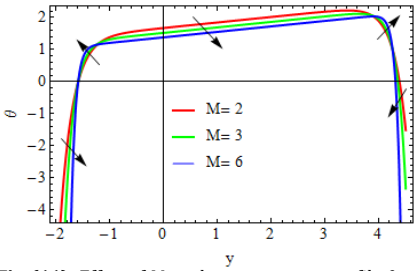

Fig. (11)- Effect of M on the temperature profile θ

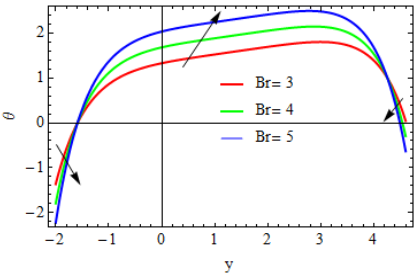

Fig. (12)- Effect of Br on the temperature profile θ

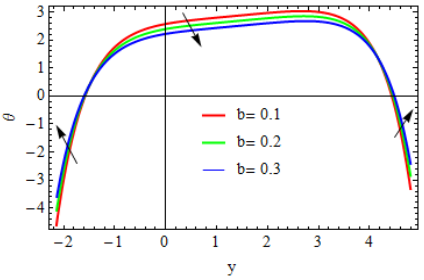

Fig. (13)- Effect of b on the temperature profile θ

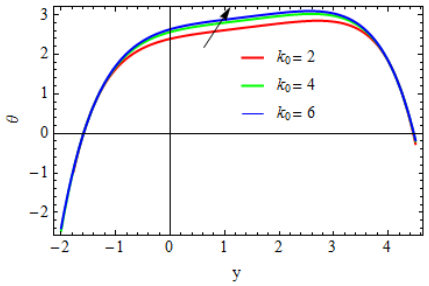

Fig. (14)- Effect of k_0 on the temperature profile θ

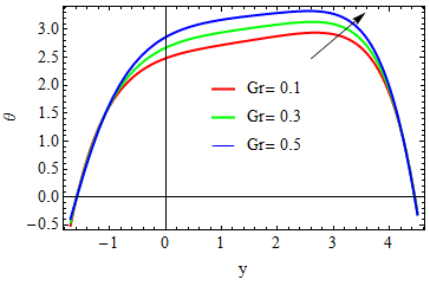

Fig. (15)- Effect of Gr on the temperature profile θ

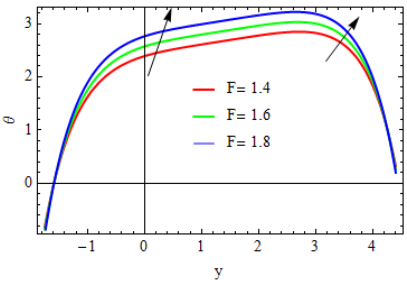

Fig. (16)- Effect of F on the temperature profile θ

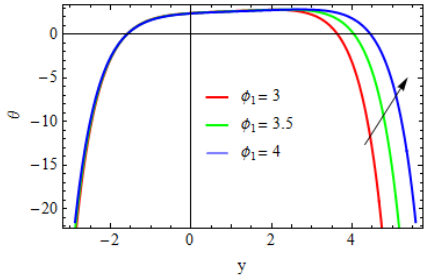

Fig. (17)- Effect of ϕ_1 on the temperature profile θ

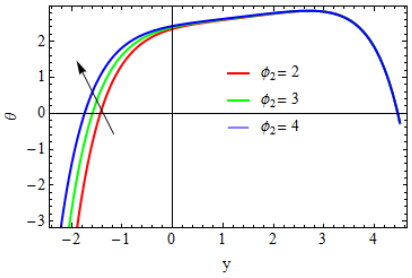

Fig. (18)- Effect of ϕ_2 on the temperature profile θ

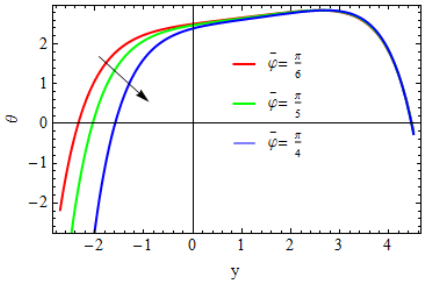

Fig. (19)- Effect of $\bar{\varphi}$ on the temperature profile θ

6.3 Concentration Distribution Ω

The graphical results for concentration profile are illustrated in figures (20-30). Opposite behavior for concentration distribution is noticed compare with the temperature distribution. Figure (20) explain that the impact of M on Ω. It is noticed that Ω exhibits oscillating behavior with an increase in M. It is observed from figures (21-24), Ω decreases in the central region and increases near the channel walls for increasing in Br, Sc, Sr and F, but opposite behavior is occurring with the increase in b, as shown in figure (25). Figures (26) and (27) deduced that Ω decreases by increasing in k_0 and Bn. Figure (28) shown that Ω decreases near the right wall and the middle part of the channel and then gradually disappear as there is no effect on Ω to the rest of the channel with an increase in ϕ_1. Figure (29) illustrated the effect of ϕ_2 on Ω. It is noticed that when an increase in ϕ_2, the concentration decreases at the left wall of the channel and merges from the central part to the rest of the channel (no effected). From figure (30) we concluded that at an increase in $\bar{\varphi}$, Ω increases at the left wall of the channel while Ω decreases at the middle portion and then gradually disappear at the right wall of the channel.

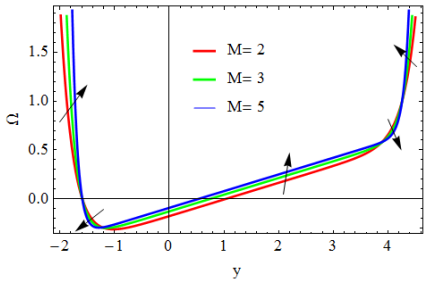

Fig. (20)- Effect of M on the concentration profile Ω

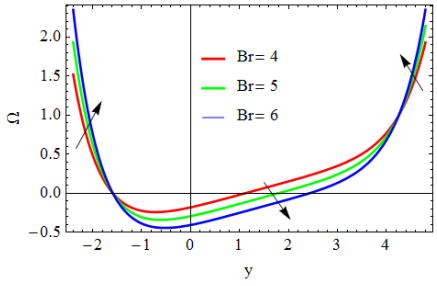

Fig. (21)- Effect of Br on the concentration profile Ω

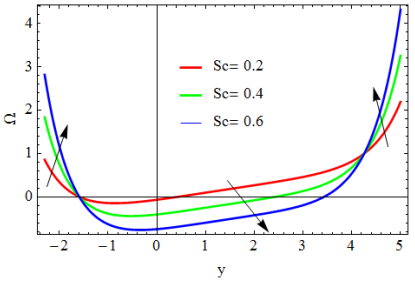

Fig. (22)- Effect of Sc on the concentration profile Ω.

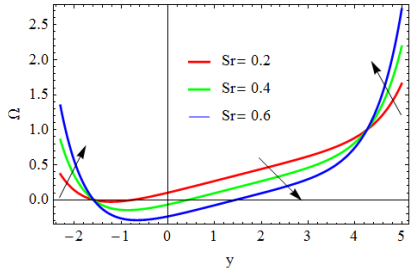

Fig. (23)- Effect of Sr on the concentration profile Ω.

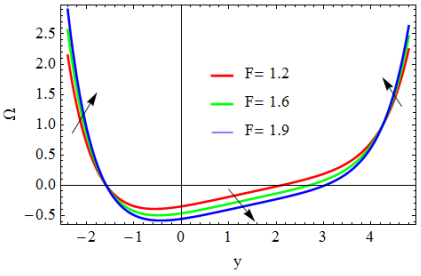

Fig. (24)- Effect of F on the concentration profile Ω.

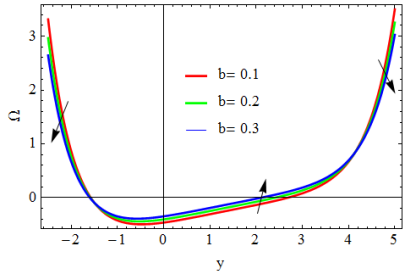

Fig. (25)- Effect of b on the concentration profile Ω.

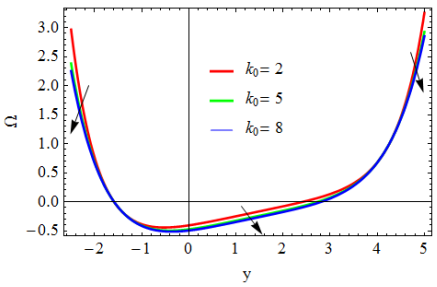

Fig. (26)- Effect of k_0 on the concentration profile Ω.

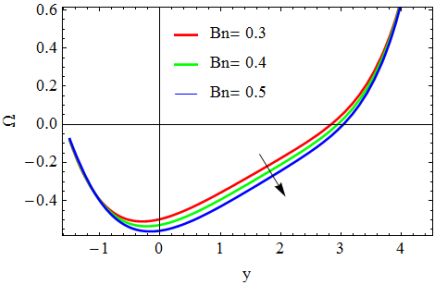

Fig. (27)- Effect of Bn on the concentration profile Ω.

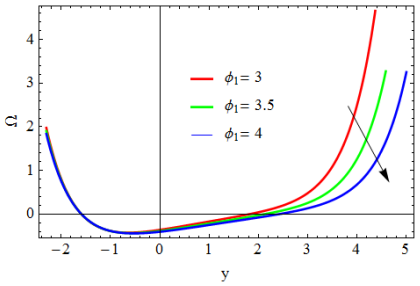

Fig. (28)- Effect of ϕ_1 on the concentration profile Ω.

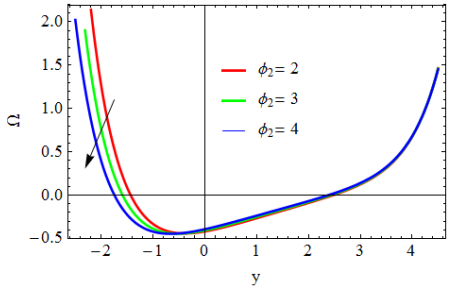

Fig. (29)- Effect of ϕ_2 on the concentration profile Ω.

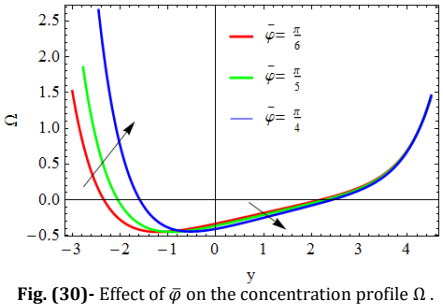

Fig. (30)- Effect of $\bar{\varphi}$ on the concentration profile Ω .

6.4 Trapping Phenomenon

The process of the formulation of an internally circulation of fluid bolus by the closed stream line in the fluid flow is called trapping phenomenon, in which the trapped bolus moves ahead with peristaltic wave. The behavior of stream function is illustrated in figures (31-39) and the stream lines near the channel do nearly strictly follow the wall waves , which are mainly engendered by the relative movement of the walls. All figures are plotted for the values $M = 0.5$, $b = 0.2, k_0 = 2, Bn = 0.001, Br = 0.6, F = 1.8,\ \bar{\varphi} = {}^{\pi}/_{4}, , \phi_1 = 0.2$ and $\phi_2 = 0.3$. We observed that the size of trapped bolus reduces with increasing M, b and $\bar{\varphi}$ whereas it enhances with increasing k_0, ϕ_1, $\phi_2$and F as shown through figures (31-37) respectively. While figure (38) shown that the increasing values of Br, it has the slight effect always negligible at the size of the trapped bolus one can see it clear of a diagram streamline. The impact of Bn is illustrate in figure (39), which shown that as Bn increases, the size of the bolus increases at the left side wall and it reduces at the right side wall of the channel. These results agree with Adnan and Abdulhadi [9]. The result for M and k_0 is also agree with Lakshminarayana et al. [1,8].

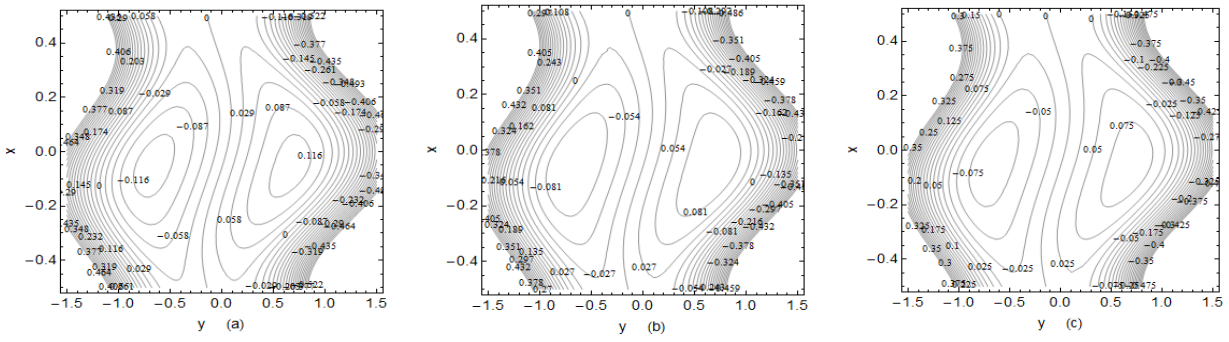

Fig. (31)- Effect of $(a)\ M = 0.5,\ (b) M = 1.5,\ (c) M = 2$ on the stream line

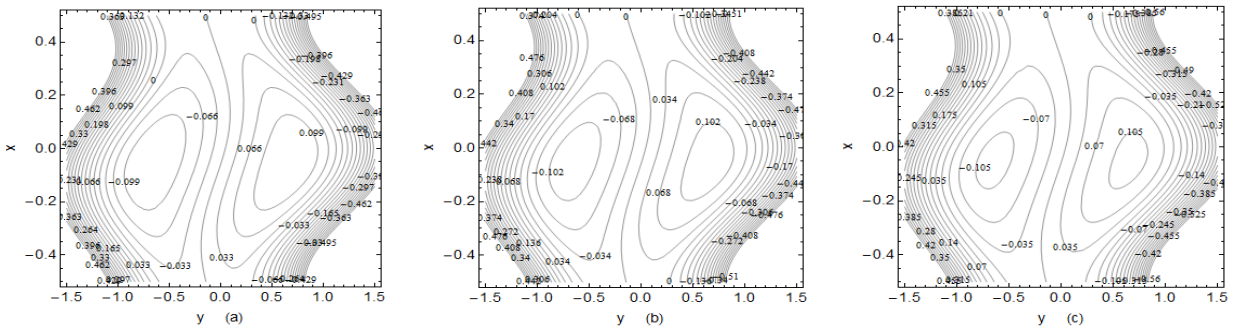

Fig. (32)- Effect of $(a)\ b = 0.2,\ (b)b = 0.3,\ (c)b = 0.4$ on the stream line

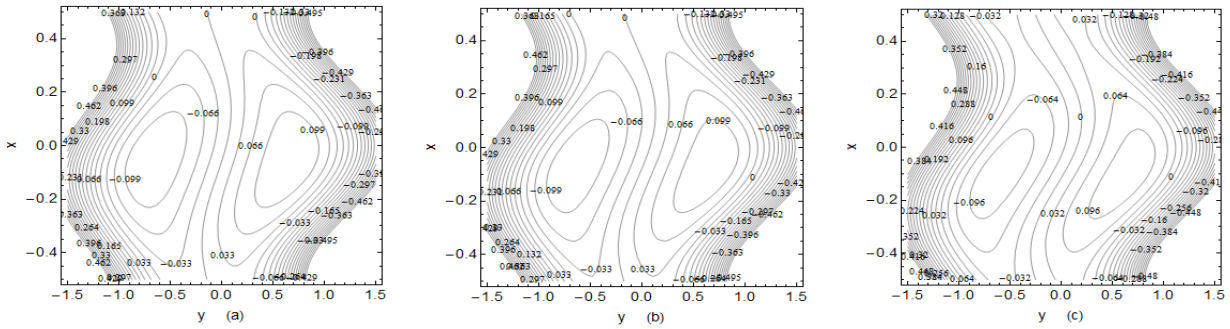

Fig. (33)- Effect of $(a)\ \bar{\varphi} = \frac{\pi}{4},\ (b)\bar{\varphi} = \frac{\pi}{3},\ (c)\bar{\varphi} = \frac{\pi}{2}$ on the stream line

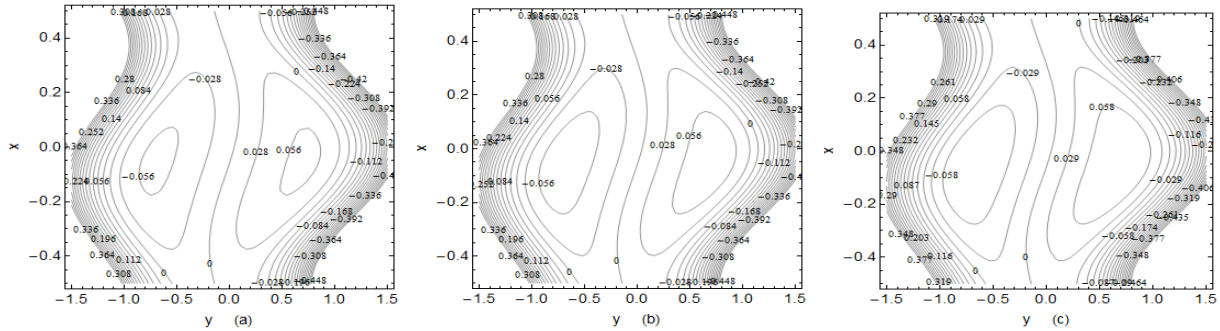

Fig. (34)- Effect of $(a)\ k_0 = 0.12,\ (b)\ k_0 = 0.15,\ (c)\ k_0 = 0.2$ on the stream line

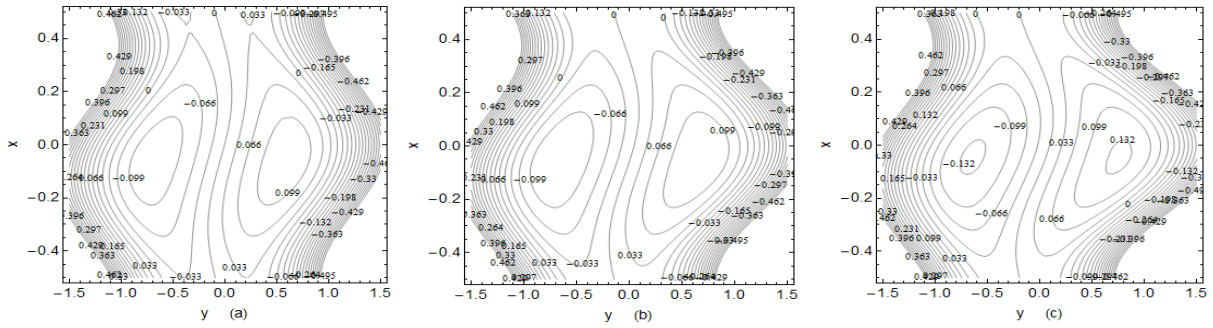

Fig. (35)- Effect of $(a)\ \phi_1 = .3,\ (b)\ \phi_1 = .4,\ (c)\phi_1 = .5$ on the stream line

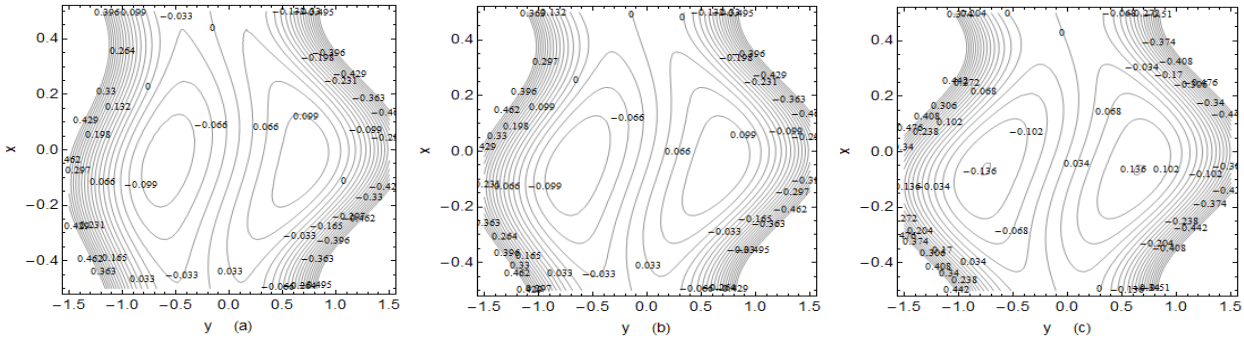

Fig. (36)- Effect of $(a)\ \phi_2 = .2,\ (b)\ \phi_2 = .3,\ (c)\phi_2 = .4$ on the stream line

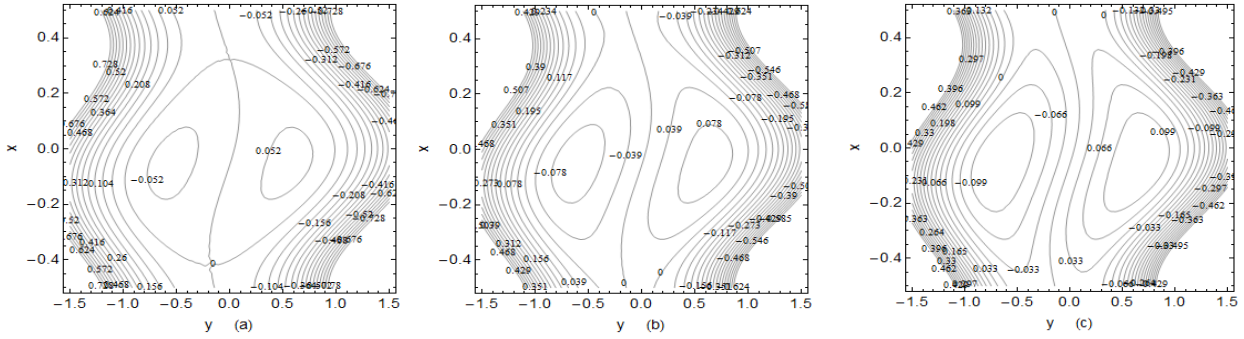

Fig. (37)- Effect of $(a)\ F = 1.6,\ (b)\ F = 1.7,\ (c)F = 1.8$ on the stream line

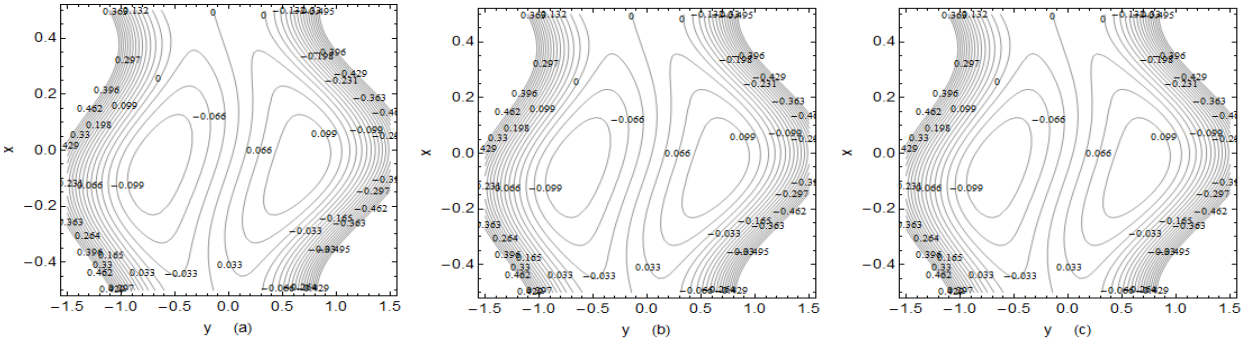

Fig. (38)- Effect of $(a)\ Br = 1,\ (b)\ Br = 10,\ (c)Br = 20$ on the stream line

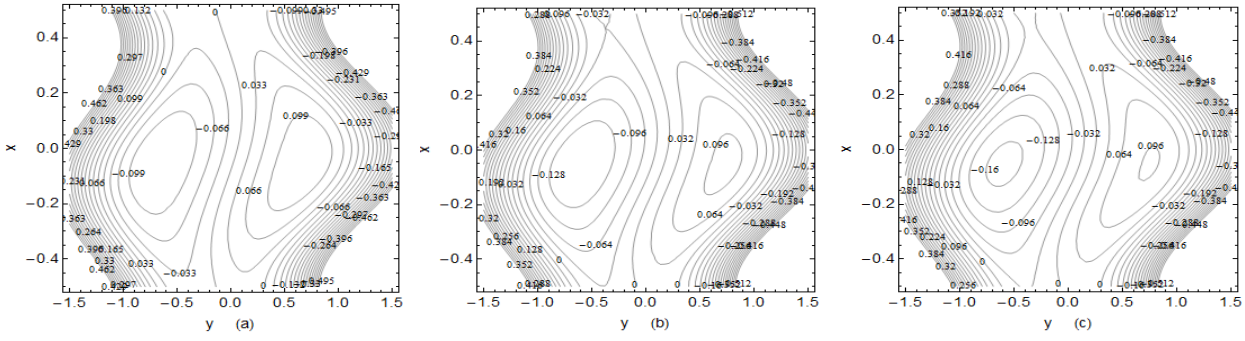

Fig. (39)- Effect of $(a)\ Bn = .1,\ (b)\ Bn = 1,\ (c)Bn = 1.3$ on the stream line

7. Conclusions

In this paper, the Influence of MHD on mixed convective heat and mass transfer analysis for the peristaltic transport of viscoplastic fluid with porous medium in tapered channel is investigated under low Reynolds number and long wavelength. The flow is considered in two-dimensional channel. the system of nonlinear partial differential equation was solved by using perturbation method. The present results have application in chemical engineering and biomedical system. In view of this study, some of the interesting conclusions are summarized as follows:

- By increasing M, the axial velocity decreases in the central region and it increases near the boundaries of the channel but the opposite occur for increasing k_0. the axial velocity increases over the whole cross-section with increasing F and it decreases by increasing b.
- The axial velocity decreases near the left wall while it increases at the center of the channel by increasing Bn. Furthermore Br has not effected on the axial velocity.
- The temperature increases with increasing k_0, Gr, Br and F.
- Opposite behavior for concentration distribution is noted compared to temperature profile. Furthermore, the concentration decreases over the whole cross-section except near the boundaries of the channel it is increases with increasing Sr and Sc.
- The temperature profile and concentration distribution exhibits oscillating behavior with increasing M.
- It is noted that the parameters ϕ_1, ϕ_2 and $\bar{\varphi}$ have similar effected on the axial velocity and temperature profile but opposite behavior accrue for concentration distribution.
- The size of trapped bolus reduces with increasing M, b and $\bar{\varphi}$ whereas it increases with increasing k_0, ϕ_1, ϕ_2 and F. Furthermore the trapped bolus increases in number and size at the left wall of the channel by increasing Bn but opposite behavior occur at the right wall.

References

[1] P. Lakshminarayana, S. Sreenadh and G. Sucharitha, "The influence of slip, wall properties on the peristaltic transport of a conducting Bingham fluid with heat transfer", *Procedia Engineering*,127(2015),1087-1094.

[2] N. Ali, K. Ullah and H. Rasool, " Bifurcation analysis for a two-dimensional peristaltic driven flow of power-law fluid in asymmetric channel", *Physics of Fluids*, 32,(2020) 073104, DIO: 10.1063/5.0011465.

[3] N. Ali and Z. Asghar, " Mixed convective heat transfer analysis for peristaltic transport of vescoplastic fluid: perturbation and numerical study", *AIP Advances* 9,(2019) 095001, DIO: 10.1063/1.5118846.

[4] S. Srinivas and M. Kothandapani, " The influence of heat and mass transfer on MHD peristaltic flow through a porous space with complaint walls. *Applied Mathematics and Computation* , 213(2009),197–208.

[5] S. Akram , S. Nadeem and A. Hussain, " Effect of heat and mass transfer on peristaltic flow of a Bingham fluid in the presence of inclined magnetic field and channel with different wave forms", *Journal of Magnetism and Magnetic Materials*, 362(2014), 184-192.

[6] K. Ramesh " Influence of heat and mass transfer on peristaltic flow of a couple stress fluid through porous medium in the presence of inclined magnetic field in an inclined asymmetric channel", *Journal of Molecular Liquids*, 219(2016),256–271.

[7] K. V. V. Satyanarayana, S. Sreenadh, G. Sucharitha and P. Lakshminarayana, " The effect of Wall Properties on the Convective Peristaltic Transport of a Conducting Bingham Fluid through Porous Medium", *Indian Journal of Science and Technology*, 9(42)(2016), 1-9.

[8] P. Lakshminarayana, K. Vajravelu, G. Sucharitha and S. Sreenadh, " Peristaltic slip flow of a Bingham fluid in an inclined porous conduit with Joule heating", *Applied Mathematics and Nonlinear Sciences*, 3(1)(2018), 41-54.

[9] F. A. Adnan and A. M. Abdulhadi, " Effect of a magnetic fluid on peristaltic transport of Bingham plastic fluid in a symmetric channel", *Science International (Lahore)*, 31(1)(2019) 29-40.

[10] M. A. Murad and A. M. Abdulhadi, " Influence of heat and mass transfer on peristaltic transport of viscoplastic fluid in presence of magnetic field through symmetric channel with porous medium", to be publish in *IOP Journal of Physics: Conference Series* in February 2021.

[11] M. R. Salman and A. M. Abdulhadi, " Effects of MHD on peristalsis transport and heat transfer with variables viscosity in porous medium", *International Journal of Science and Research*, 7(2)(2018),612-623.

[12] J.C. Misra, B. Mallick and A. Sinha, " Heat and mass transfer in asymmetric channels during peristaltic transport of an MHD fluid having temperature-dependent properties", *Alexandria Engineering Journal*, 57(2018), 391-406.

[13] T. Hayat, S, Noreen, M. Shabab Alhothuali, S. Asghar and A. Alhomaidan, " Peristaltic flow under the effect of an induced magnetic field and heat and mass transfer", *International Journal of Heat and Mass Transfer*, 55(2012),443-452.